

VTrans: Accelerating Transformer Compression with Variational Information Bottleneck based Pruning

Oshin Dutta¹ Ritvik Gupta² Sumeet Agarwal¹

¹ Indian Institute of Technology, Delhi

² Carnegie Mellon University

oshin.dutta@ee.iitd.ac.in, ritvikgu@cs.cmu.edu, sumeet@iitd.ac.in

Abstract

In recent years, there has been a growing emphasis on compressing large pre-trained transformer models for resource-constrained devices. However, traditional pruning methods often leave the embedding layer untouched, leading to model over-parameterization. Additionally, they require extensive compression time with large datasets to maintain performance in pruned models. To address these challenges, we propose **VTrans**, an iterative pruning framework guided by the Variational Information Bottleneck (VIB) principle. Our method compresses all structural components, including embeddings, attention heads, and layers using VIB-trained masks. This approach retains only essential weights in each layer, ensuring compliance with specified model size or computational constraints. Notably, our method achieves upto 70% more compression than prior state-of-the-art approaches, both task-agnostic and task-specific. We further propose faster variants of our method: **Fast-VTrans** utilizing only 3% of the data and **Faster-VTrans**, a time efficient alternative that involves exclusive finetuning of VIB masks, accelerating compression by upto 25 times with minimal performance loss compared to previous methods. Extensive experiments on BERT, ROBERTa, and GPT-2 models substantiate the efficacy of our method. Moreover, our method demonstrates scalability in compressing large models such as LLaMA-2-7B, achieving superior performance compared to previous pruning methods. Additionally, we use attention-based probing to qualitatively assess model redundancy and interpret the efficiency of our approach. Notably, our method considers heads with high attention to special and current tokens in un-pruned model as foremost candidates for pruning while retained heads are observed to attend more to task-critical keywords.

1 Introduction

Since their inception, Transformers (Vaswani et al., 2017) have fundamentally transformed the NLP field, offering pre-trained self-supervised models adaptable to specific downstream tasks (Wang et al., 2018). However, the surge in popularity and scale of Transformer models has amplified deployment challenges on resource-constrained devices, attributed to elevated latency and substantial storage demands (Raffel et al., 2020; Brown et al., 2020).

This has motivated extensive work in transformer pruning focusing on various components such as layers, heads, blocks within weight matrices, and hidden states. However, embeddings, which account for over 22% of total model parameters, are often overlooked (Xia et al., 2022; Hou et al., 2020) due to challenges in maintaining consistency with skip connection. Moreover, existing methods often use magnitude-based (Han et al., 2015) or simply sparsity-based pruning (Xia et al., 2022), which overlooks the importance of weights for the given task.

An alternative approach to achieving compact yet high-performing models is knowledge distillation (Hinton et al., 2015), where insights from a larger teacher model are transferred to

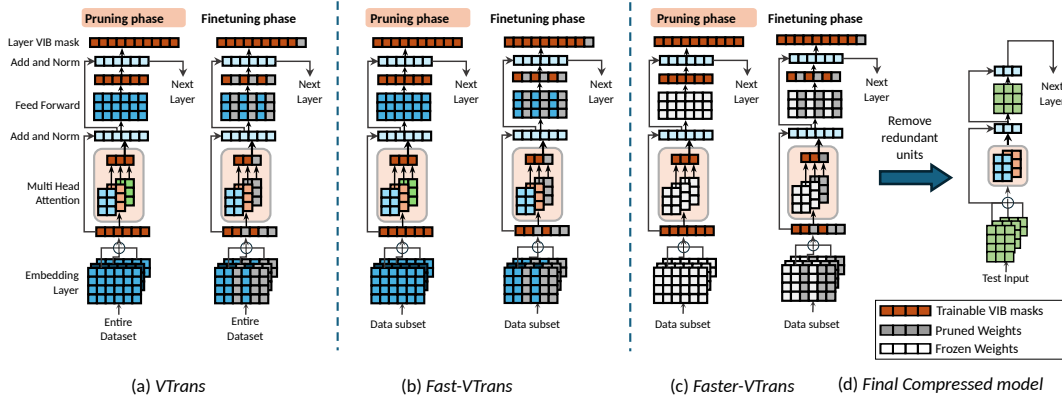


Figure 1: (a) Our primary method - *VTrans* involves training all pre-trained model parameters and VIB masks on the entire dataset during pruning, but during finetuning, only the unmasked important weights are updated. (b) *Fast-VTrans* utilizes a subset of data for both pruning and finetuning. (c) *Faster-VTrans*, the fastest among all, trains VIB masks, Add Norm layer, and model bias parameters during pruning and finetuning, using only a subset of the entire dataset. (d) The masked and redundant units are removed after the finetuning phase, resulting in the dense compressed model.

a carefully designed smaller student model. However, task-agnostic knowledge distillation can incur a prohibitively high computational cost (Jiao et al., 2019). Quantization is another effective approach that achieves high compression and speedup with minimal loss in performance by leveraging techniques such as quantization-aware training (Bai et al., 2021; Kim et al., 2021; Zafir et al., 2019).

To address the challenges, we propose a novel transformer pruning method based on the Variational Information Bottleneck (VIB) principle. It effectively removes redundant elements while preserving information flow. Additionally, we leverage knowledge distillation to achieve higher pruning ratios without sacrificing performance.

Our contributions are:

- We propose a structured pruning framework for transformers that is evaluated in both task-specific and task-agnostic contexts, while adhering to user-defined constraints on either model parameters or FLOPs.
- Unlike prior methods, we extend compression to embedding states, alongside other structural components like layers, attention heads, and feedforward networks (FFN) enabling higher compression levels.
- We propose two alternative - *Fast* and *Faster* approaches (Figure 1) to the main compression method which are both time and resource efficient with minimal performance degradation compared to previous approaches.
- We evaluate the proposed methods on GLUE and SQuAD tasks while compressing BERT, ROBERTa and GPT-2 pre-trained models with superior performance to previous SOTA (Figure 2).
- Furthermore, we establish the scalability of our method by pruning and evaluating LLaMA-2 with 7 billion parameters on WikiText-2 dataset (Table 1).

2 Related Work

Pruning. It involves removing redundant model parameters for substantial model compression with minimal performance loss (Xia et al., 2022; Zhu & Gupta, 2017; Zafir et al., 2021; Renda et al., 2020; Liang et al., 2023b). Recent techniques for transformer model pruning employ structured approaches, targeting specific components like layers (Fan et al., 2020; Sajjad et al., 2020), heads (Michel et al., 2019; Voita et al., 2019; Liang et al., 2021),

intermediate dimensions (McCarley et al., 2021; Wang et al., 2020c) and blocks of weight matrices (Lagunas et al., 2021) or multiple components jointly (Xia et al., 2022; Sun et al., 2023). Low-rank approximation has also been combined with pruning (Li et al., 2023) to further compression. But these prior methods do not prune embedding parameters which often form more than 20% of the total parameters. Methods utilizing only forward pass during pruning (Sun et al., 2023) often involve semi-structured pruning that cannot be made dense post-pruning, leading to slower inference speeds. Certain pruning methods focus only on task-agnostic Liang et al. (2023a) and some on task-specific Nasery et al. (2023); Yang et al. (2022).

Knowledge distillation. Another compression method involves training smaller (student) model from a larger (teacher) model. The technique has found applications in both, task-specific (Tang et al., 2019; Turc et al., 2019; Aguilar et al., 2020) as well as task-agnostic domains (Sanh et al., 2020a; Khanuja et al., 2021; Chen et al., 2021). In addition, recent advancements (Sun et al., 2019; 2020; Hou et al., 2020; Romero et al., 2015) have extended its application by enabling the incorporation of information from intermediate layers into the student model’s training. Moreover, studies (Ma et al., 2023; Sanh et al., 2020b) demonstrate the effectiveness of combining pruning with knowledge distillation. However, these methods often entail extensive training time.

Variational Information Bottleneck. It approximates (Alemi et al., 2016) the information bottleneck principle (Slonim & Tishby, 1999; Tishby & Zaslavsky, 2015), focusing on extracting relevant information from input variables for output variables. It aims to maximize mutual information between intermediate layers and outputs while minimizing inter-layer mutual information to eliminate redundancy in information. It has been successfully applied to remove neurons in CNN (Dai et al., 2018) and to RNN models (Srivastava et al., 2021). Henderson & Fehr (2022) formulate a non-parameteric variational autoencoder with VIB for transformers, but it is not aimed at pruning weights. In our work, we apply the principle for transformer compression.

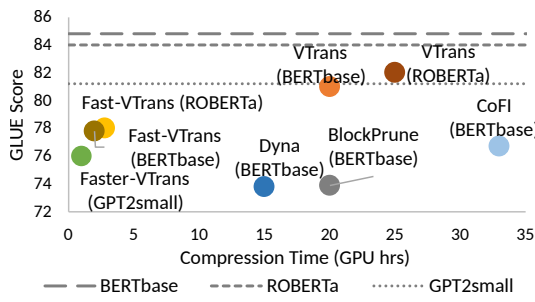


Figure 2: Our method surpasses previous techniques in compressing BERT-base, ROBERTa-base, and GPT-2-small models. Our faster variants have reduced compression timeframes. All models have 28M parameters being compressed from their respective teachers.

Model	Size	PPL	Inference Speedup
LLaMA-2	7B	5.11	1×
Wanda 2:4	3B	10.52	1.14×
Bonsai	3B	19.47	1.58×
LLM-pruner	3B	19.24	1.5×
Faster-VTrans	3B	11.8	1.82×

Table 1: Pruned models evaluated on Wikitext-2. Our method outperforms structured pruning (Bonsai and LLM-pruner) and achieves faster inference than semi-structured pruning (Wanda 2:4).

3 Background

3.1 Basic Transformer Architecture

Transformer network $f(\cdot; \theta_s)$ parameterised by θ_s used for NLP tasks typically consist of an embedding module and L layers with each layer containing Multi-Head Attention (MHA) module and two Feed Forward Networks (FFN). We denote the input to a transformer network as $x \in \mathbb{R}^d$ and the associated label as $y \in \mathcal{Y}$. Further, we represent the embedding layer hidden states obtained after the addition of positional and input embeddings as \mathbf{m} , output of MHA activations as $\{\mathbf{a}_i\}_{i=1}^L$ and FFN layer embedding as $\{\mathbf{h}_i\}_{i=1}^L$.

3.2 Compressed Representations with Variational Information Bottleneck

Tishby & Zaslavsky (2015) and Dai et al. (2018) conceptualised successive layer representations in a deep neural network to form a Markov chain while treating the input as a stochastic variable. In the context of transformers, we extend it to the successive output representations from the embedding layer, Multi-Head Attention (MHA) layers, and Feed-Forward Network (FFN) layers. Our objective is to obtain condensed intermediate representations or activations \tilde{k}_i after each module (embedding layer, MHA, FFN) in the transformer architecture while preserving essential information in the predicted output \tilde{y} . Unlike the compressed FFN representation as formulated in Dai et al. (2018), $k_i \in \mathbb{R}^{n \times seq \times d}$, $\tilde{k}_i \in \mathbb{R}^{n \times seq \times d'}$ are each sets of vectors with n input examples and seq tokens and d' represents the compressed d dimension. As done by Dai et al. (2018), we frame the optimization problem as: $\mathcal{L}_i = \beta_i I(\tilde{k}_i, k_{i-1}) - I(\tilde{k}_i, Y)$. Here, $I(\cdot)$ denotes mutual information between two random variables and β_i is a hyper-parameter controlling the trade-off between compression and prediction accuracy. To simplify notation, we denote the compressed version \tilde{k} as k .

To make the problem tractable, we invoke the variational upper bound as done by Alemi et al. (2016),

$$\tilde{\mathcal{L}}_i = \mathbb{E}_{X, Y, k_i, k_{i-1}} \left[\beta_i \mathbb{D}_{KL} \left[p(k_i | k_{i-1}) \| q(k_i) \right] - \log q(y | k_L) \right] \geq \mathcal{L}_i \quad (1)$$

Here, $q(k_i)$ and $q(y | k_L)$ approximate $p(k_i)$ and $p(y | k_L)$, respectively. We get the compressed representations by performing a dot product of the transformer activations with a random set of vectors $z_i \in \mathbb{R}^{n \times seq \times d}$, where $z_i = \mu_i + \epsilon_i \odot \sigma_i$. $\mu_i \in \mathbb{R}^{1 \times d}$, $\sigma_i \in \mathbb{R}^{1 \times d}$ are learnable parameters, while $\epsilon_i \in \mathbb{R}^{n \times seq \times d}$ is sampled from non-parameterized $\mathcal{N}(\mathbf{0}, \mathbf{I})$, thus broadcasting μ_i and σ_i .

$$k_i = z_i \odot f_i(k_{i-1}) \quad ; z_i \in \mathbb{R}^{n \times seq \times d} \quad (2)$$

$f(\cdot)$ denotes a standard sub-layer of the transformers like the value head projection or the up projection sub-layer. Following Dai et al. (2018), we derive the final VIB objective function as,

$$\tilde{\mathcal{L}}_{\text{VIB}} = \sum_i^L \beta_i \sum_{j=1}^{r_i} \log \left(1 + \frac{\mu_{i,j}^2}{\sigma_{i,j}^2} \right) - \mathbb{E}_{X, Y, k} [\log q(y | k_L)] \quad (3)$$

where r_i denotes the total hidden states or neurons within layer i . The expectation is approximated with the task classification layer. Unlike the application of VIB on non-transformer-based networks as done by Dai et al. (2018), compressing one token's representation in transformer-based models can inadvertently affect the representations of other tokens due to their inter-dependencies. However, by sampling a random vector with the shape $(samples, sequence_length, dimensions)$, each token's representation can be uniquely adjusted by its own random vector. This approach potentially preserves more detailed context and dependencies, maintaining the integrity of the token-level information.

4 Method

Our approach involves two phases: **pruning** and **finetuning**.

During pruning, we systematically prune the student model, initialized from the finetuned teacher, using VIB-based pruning while distilling knowledge from the teacher model. In the finetuning phase, we optimize the remaining model parameters and VIB masks to achieve the final compressed model with optimal performance. We elaborate on the primary method in section 4.1, and discuss the *Fast* and *Faster* variants in sections 4.3.

4.1 VIB-based Pruning

Following Equation 2, we define compressed representations for each structural module in a transformer by multiplying the output of the module element-wise to a random vector. The

Model	Pars (Mil)	SST-2 (Acc)	QNLI (Acc)	MNLI (Acc)	QQP (Acc)	CoLA (M. Corr)	RTE (Acc)	STS-B (P. Corr)	MRPC (Acc)	Avg Score	Prune Time (GPU hrs)
BERT _{base} (teacher)	109	93.1	91.5	84.5	91.1	61.2	79.8	89.3	88.3	84.8	-
DynaBERT (Hou et al., 2020)	34	89.4	83.9	76.3	88.8	15.8	66.4	85.4	84.6	73.8	~ 15
BlockPrune (Lagunas et al., 2021)	28	89.3	84.7	78.8	88.8	15.8	66.4	85.4	81.9	73.9	~ 20
CoFi (Xia et al., 2022)	28	90.6	86.1	80.6	90.1	35.6	64.7	83.1	82.6	76.7	~ 33
PostPrune (Kwon et al., 2022)	28	75.7	63.8	45.5	67.5	32.4	58.6	80.2	78.7	62.8	~ 0.08
VTrans (ours)	28*	92.2	89.7	83.8	90.5	43.3	73.4	87.9	87.0	81.0	~ 20
Fast-VTrans (ours)	28*	90.8	85.8	79.3	89.2	37.6	68.0	87.9	83.8	77.8	~ 2
Faster-VTrans (ours)	28*	82.3	81.8	72.1	81.4	36.3	67.6	86.8	82.5	73.9	~ 0.7
RoBERTa _{base} (teacher)	124	95.3	93.2	87.7	73.8	62.0	78.7	91.2	90.1	84.0	-
MINILMv2 ₆ (Wang et al., 2020b)	82	93.5	91.6	84.3	72.8	57.8	72.1	87.5	88.2	81.0	~ 300
FeatureCorr (Huang et al., 2023)	82	93.8	92.0	85.6	73.5	60.3	72.5	88.3	89.6	82.0	-
VTrans (ours)	82*	94.8	93.0	87.3	73.6	61.0	73.1	90.9	90.1	83.0	~ 25
Fast-VTrans (ours)	82*	94.1	91.9	85.4	72.9	60.4	72.7	89.6	89.8	82.1	~ 2.8
Faster-VTrans (ours)	82*	93.4	90.6	84.8	72.3	59.2	72.6	87.9	88.5	81.2	~ 1
GPT _{2small} (teacher)	125	92.7	88.5	82.3	89.7	47.4	74.4	88.9	85.8	81.2	-
DistilGPT2 (Sanh et al., 2020a)	82	90.7	87.9	81.6	66.8	39.4	68.3	79.6	87.9	75.3	~ 300
FeatureCorr (Huang et al., 2023)	82	92.0	88.5	83.4	70.6	42.3	70.2	81.6	88.4	77.1	-
VTrans (ours)	82*	92.4	88.8	82.8	89.5	45.4	72.9	88.1	86.0	80.7	~ 25
Fast-VTrans (ours)	82*	92.0	88.4	82.8	88.7	43.5	71.4	86.5	86.0	80.0	~ 2.8
Faster-VTrans (ours)	82*	91.9	87.3	80.1	86.2	42.1	70.8	86.5	86.0	78.9	~ 1

Table 2: The performance of models on GLUE dataset. * indicates the average number of parameters across all datasets. Average variance in performance of our models is about $\pm 0.4\%$ obtained over five random initial seeds.

compressed embedding representation is thus defined as $\mathbf{m} = \mathbf{z}_m \odot \text{Emb}(X, W)$, where \mathbf{z}_m is the random vector multiplied element-wise to the output of the embedding layer. W denote the weight matrices of the embedding layer. Similarly, for layer i the compressed MHA representation is defined as $\mathbf{a}_i = \mathbf{z}_{a_i} \odot [\text{Att}_1, \text{Att}_2, \dots, \text{Att}_J]$, compressed FFN representation as $\mathbf{h}_i = [\text{gelu}(XW_{iU}) \text{diag}(\mathbf{z}_{\text{inter},i}) \cdot W_{iD}] \odot \mathbf{z}_{\text{out},i}$, where $W_{iU} \in \mathbb{R}^{r_i \times r_f}$ and $W_{iD} \in \mathbb{R}^{r_f \times r}$ are intermediate up-projecting and final down-projecting layer matrices respectively.

Layer pruning. We incorporate the ability to prune whole MHA and FFN layers by introducing additional random vector \mathbf{z}_{layer} . This enables effective pruning in scenarios with high sparsity requirements. Thus, the MHA and FFN representation for layer i are defined as $MHA_i = \mathbf{z}_{layer,i} \cdot (\mathbf{a}_i \cdot W_i^O)$; $FFN_i = \mathbf{z}_{layer,i} \cdot \mathbf{h}_i$, where $W_i^O \in \mathbb{R}^{r_i}$ denotes the output attention matrix.

Implementation of masks for pruning. The $\mu_{i,j}$ and $\sigma_{i,j}$ parameters of the $\mathbf{z}_{i,j}$ vectors of layer i and neuron j are initially sampled from normal distributions and iteratively refined during pruning. As shown by Dai et al. (2018), at the minima of the Equation 2, whenever $\alpha_{i,j} = \mu_{i,j}^2 / \sigma_{i,j}^2 = 0$, then that neuron j of layer i is redundant. In the inference phase, these $\mathbf{z}_{i,j}$ vectors are converted to hard masks $\mathbf{z}_{i,j}^{mask}$ using a thresholding operation on $\alpha_{i,j}$ for pruning neurons as defined by,

$$z_{i,j}^{mask} = \begin{cases} 0 & \text{if } \log \frac{\mu_{i,j}^2}{\sigma_{i,j}^2} \leq \tau \\ 1 & \text{if } \log \frac{\mu_{i,j}^2}{\sigma_{i,j}^2} > \tau \end{cases} \quad (4)$$

Sparsity Control. Using $\mathbf{z}_{i,j}^{mask}$ hard masks, we calculate model sparsity as the ratio of pruned parameters to the initial count. For FLOPs constraints, sparsity represents the reduction ratio in FLOPs to the initial value. We adopt an approach akin to Xia et al. (2022); Dutta et al. (2023) to incorporate a Lagrangian term which enhances stability and provides finer control over pruning by enforcing an equality constraint $s_e = t$ and introducing a violation penalty as $\mathcal{L}_s = \lambda_1 \cdot (s_e - t) + \lambda_2 \cdot (s_e - t)^2$, where s_e is the expected model sparsity, t is the target sparsity and $\lambda_1, \lambda_2 \in \mathbb{R}$ are Lagrangian multipliers jointly updated during the pruning process. We compute s_e by employing the sigmoid differentiable form of $\mathbf{z}_{i,j}^{mask}$.

4.2 Knowledge Distillation

We distill knowledge from the original full-sized Transformer to the student model during pruning by minimizing the cross entropy between their output probability distributions \mathbf{p}_s

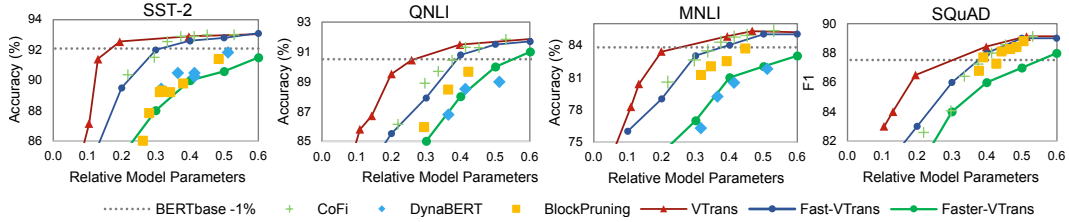


Figure 3: Pruning BERT-base (teacher model) on GLUE and SQuAD tasks: Each point denotes the mean performance of pruned models averaged over five random trials with different seeds with average variance of $\pm 0.4\%$ across all models. The dashed line represents a 1% performance drop from the teacher model.

and \mathbf{p}_t as $\mathcal{L}_{\text{pred}} = D_{\text{KL}}(\mathbf{p}_s \parallel \mathbf{p}_t)$. We also adopt a layer-wise distillation approach inspired by Xia et al. (2022). This method aligns the teacher’s layer with the evolving student’s, defining an intermediate distillation loss function as $\mathcal{L}_{\text{layer}} = \sum_{i \in \mathcal{T}} \text{MSE}(W_{\text{layer}} \mathbf{H}_s^{m(i)}, \mathbf{H}_t^i)$

where W_{layer} is a transformation matrix initialized to identity. $\mathbf{H}_s^{m(i)}$ and \mathbf{H}_t^i represent the student’s and teacher’s hidden layer representations, respectively, for layer distillation, with $m(\cdot)$ mapping teacher layer representations to the closest student layer as $m(i) = \arg \min_{j: \text{unpruned layers}} \text{MSE}(W_{\text{layer}} \mathbf{H}_s^j, \mathbf{H}_t^i)$. Hence, the distillation loss encompasses both

the layer-wise loss and the logit-based cross entropy loss with η controlling their relative influence: $\mathcal{L}_{\text{distil}} = \eta \mathcal{L}_{\text{pred}} + (1 - \eta) \mathcal{L}_{\text{layer}}$. The comprehensive loss function to be minimised during pruning is $\mathcal{L}_{\text{total}} = \mathcal{L}_{\text{distil}} + \hat{\mathcal{L}}_{\text{VIB}} + \mathcal{L}_s$. The steps of the our method is reiterated in Algorithm 1 in the Appendix.

4.3 Faster variants of our method

Faster compression with Data Subset. Leveraging the valuable features and patterns learned during the initial training phase, our *Fast-VTrans* approach involves training VIB masks and refining un-masked pre-trained model parameters with a significantly reduced data requirement as shown in figure 1(b). Intuitively, this process is expected to facilitate adaptation to lower model parameters without overfitting. To achieve this, we employ a 3% data subset for pruning and fine-tuning, balancing efficiency and adaptability.

VIB mask training. Motivated by the recent advancements in post-training pruning methodologies (Kwon et al., 2022), we propose the fastest variant, *Faster-VTrans* that freezes all pre-trained model parameters (Figure 1(c)). During pruning, only VIB masks are trained to target irrelevant elements. Additionally, all norm and bias terms (where available) are fine-tuned to compensate for information loss. This approach, using only 3% of the data, significantly reduces compression time while maintaining performance, making it ideal for scenarios with limited time or resources.

5 Experiments

5.1 Implementation Details

Datasets. We assess the efficacy of our proposed method across a comprehensive set of linguistic understanding tasks - the General Language Understanding Evaluation (GLUE) benchmark (Wang et al., 2018), Stanford Question Answering Dataset (SQuAD) version 1.1 (Rajpurkar et al., 2016) and WikiText-2 (Merity et al., 2016).

Baseline Models. We compare our method variants with several previous techniques: DynaBERT (Hou et al., 2020), Block Pruning (Lagunas et al., 2021), PostPrune (Kwon et al., 2022), CoFi (Xia et al., 2022), FeatureCorr (Huang et al., 2023), DistilBERT (Sanh et al., 2020a), TinyBERT-GD (Jiao et al., 2019), MiniLM (Wang et al., 2020b), and HomoBERT (Liang et al.,

2023a). We also compare our pruned LLaMA-2 models with previous semi-structured pruning techniques- SparseGPT (Frantar & Alistarh, 2023), Wanda (Sun et al., 2023) and structured pruning techniques- LLM-pruner (Ma et al., 2023), Bonsai (Dery et al., 2024). Details are deferred to Appendix A.2.

Training Details. The primary method utilizes entire datasets for pruning and finetuning, while the *Fast* and *Faster* variants operate on a randomly sampled subset, approximately 3% of the data. For *Fast* and *Faster* variants, 8000 samples are used for pruning and finetuning on large datasets and 2000 on smaller ones of GLUE and SQuAD. Finetuning uses 16000 samples for large datasets and the entire dataset for smaller ones. We conduct five runs with random seeds for each sparsity constraint, reporting average performance. Experiments conducted to come to the final hyper-parameter settings are provided in Appendix A.5.

5.2 Evaluation

Performance comparison and Compression speedup. In Table 2, we compare pruned models derived from our primary method and its faster variants (*Fast* and *Faster*) with alternative distillation and pruning approaches. Our process starts from three teachers - BERTbase, ROBERTa, and GPT-2 small. To ensure a fair comparison of performance on GLUE datasets and compression time (measured on the largest dataset MNLI) with previous methods that share the same teacher model, we categorize the obtained models into three sections. In the uppermost group, we compare models with 28 million parameters and 75% sparsity to match previous smallest models (Xia et al., 2022). Our primary method outperforms prior techniques with similar order of compression time. *Fast-VTrans* shows a 16x acceleration compared to CoFi, and *Faster-VTrans* is at least 20x faster than DynaBERT and BlockPrune, with similar performance. Although PostPrune (Kwon et al., 2022) takes lower compression time, our method yields stable performance across different seed initialization (Appendix B.2). In the middle group, our 66% sparse model by *VTrans*, outperforms both MINILMv2 and FeatureCorr, which utilize six-layer student models, with a 1% higher GLUE score. Additionally, the faster variants demonstrate comparable performance with substantially reduced compression time. Finally, in the bottom group, when applied to the decoder-based GPT-2-small model, our compression technique demonstrates superior performance over previous approaches with minimal compression time. Furthermore, our pruned model compressed from a larger model- uncased BERT-large- outperforms DistilBERT and MINILMv2 on two GLUE tasks while achieving comparable results on the remaining tasks (Appendix B.3).

Model Size and Performance comparison. In Figure 3, we compare the performance of the models obtained with our task-specific approaches with previous methods across various sparsity levels in terms of relative model parameters. We note that our primary approach is able to achieve about 70 to 80% compressed models with less than 1% loss in accuracy from the un-pruned teacher model over all the tasks. It achieves about 20 to 70% higher sparsity than other pruning methods like CoFi, BlockPruning and DynaBERT as it can prune embedding states along with intermediate layers, heads and hidden units unlike others. The faster variants of our method retain performance comparable to previous approaches but with 10 to 20x speedup in compression as seen in Table 2.

Task-agnostic performance. To evaluate our primary method on task-agnostic setting, we use general distillation during pruning and obtained a compressed model of similar size as obtained by previous approaches (Liang et al., 2023a; Jiao et al., 2019). We finetune the model on each of the tasks in GLUE and report results of four of the tasks in Table 3. Our model performs better on three of the four tasks than other models obtained with previous task-agnostic approaches such as TinyBERT, MiniLM and HomoBERT.

Model	Parameters (Million)	SST-2 (Acc)	QQP (Acc)	MRPC (Acc)	MNLI (Acc)
BERT _{base}	109	93.1	91.1	88.3	84.5
TinyBERT ₄	14.5	89.7	90.0	81.4	80.4
MinilM ₃	17.0	89.3	88.8	81.9	78.8
HomoBERT	14.1	90.1	89.9	87.3	81.2
<i>VTrans</i> w GD	14.5	91.8	90.3	87.8	80.6

Table 3: The performance of models pruned using task-agnostic general distillation (GD) on GLUE: The pruned models are fine-tuned on downstream tasks. TinyBERT results are reported without data augmentation for fair comparison.

	QNLI (60%)		MNLI (60%)		QNLI (95%)		MNLI (95%)		SQuAD (60%)		SQuAD (95%)	
	Speedup	Acc										
Our Method	1.5 \times	91.5	1.5 \times	84.3	9 \times	81.9	9 \times	74.2	1.4 \times	87.0	7 \times	79.6
-Embeddings	1.7 \times	90.2	1.5 \times	83.9	9.2 \times	80.6	9.4 \times	73.5	1.4 \times	84.3	7.5 \times	77.6
-Layers	1.5 \times	91.5	1.5 \times	84.2	7 \times	81.9	7 \times	73.8	1.4 \times	85.8	5 \times	78.0
-Embeddings & Layers	1.5 \times	90.2	1.5 \times	83.9	6 \times	80.4	6 \times	72.6	1.4 \times	84.5	5 \times	75.8

Table 4: Investigating Pruning Strategies in BERT for varied sparsity constraints in GLUE and SQuAD Tasks: Removing embedding masks results in a performance decline. Removing layer masks reduces speedup, while removing both increases pruning of hidden states and heads, ultimately leading to diminished performance and reduced speedup in high sparsity models.

Method	WikiText2 \downarrow PPL	BoolQ Acc	PIQA Acc	HellaSwag Acc	WinoGrande Acc	ARC-e Acc	ARC-c Acc	Average \uparrow Acc	Prune Time(hrs)
Unpruned model	5.68	76.5	79.8	76.1	70.1	72.8	47.6	70.48	-
LLM-Pruner \dagger	16.41	60.28	69.31	47.06	53.43	45.96	29.18	45.95	1
LoRAPruner \dagger	11.60	61.88	71.53	47.86	55.01	45.13	31.62	52.17	> 24
Bonsai	10.92	67.22	60.85	43.09	61.64	54.92	26.28	52.33	40
Faster-VTrans\dagger	10.58	63.27	68.56	42.0	57.38	56.97	26.46	52.44	2

Table 5: Zero shot performance of the compressed LLaMA-7B. \dagger Finetuned with LoRA . Our method takes 10 to 20 times lower time to prune than other methods with similar performance. Method with lower compression time have much lower average performance.

5.3 Feasibility of Compression with Faster Variants

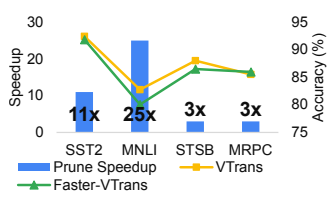


Figure 4: Speeding-up Compression: *Faster-VTrans* achieves significant speed-up over *VTrans* on GLUE tasks, with minimal performance loss for models performance to a significant degree. 35% smaller than GPT-2_{small}.

Influence of data-subset on performance. To explore the relationship between data sample size and compression performance, we conducted pruning experiments across GLUE tasks. In our trials, we used 8000 samples for larger datasets like MNLI, QQP, SST2, and QNLI, and 2000 samples for smaller datasets such as MRPC, STSB, CoLA, and RTE. Interestingly, increasing sample size for larger datasets in the faster variant led to a 1% performance boost, but at the expense of compression times 2 to 4x longer (Appendix A.3). This suggests the viability of compressing pre-trained models with limited datasets, while maintaining crucial characteristics and preserving performance to a significant degree.

Pruning Speedup in Decoder Models. In order to assess the compression speedup for decoder models, we employ our primary method and the *Faster* variant to compress GPT-2_{small}. We compare the performance and speedup with both the methods across four GLUE datasets. Notably, on large datasets such as MNLI and SST-2, as depicted in Figure 4, there is a substantial speedup (ranging from 11 to 25x) in compression achieved with *Faster-VTrans*, while incurring less than 3% accuracy degradation compared to our primary method.

5.4 Scaling-up to prune more than billion parameters

We apply our *Faster-VTrans* variant without distillation to remove redundant units from the LLaMA-2 7 billion model. Table 1 displays our model’s (1.6 \times) higher inference speedup compared to Wanda (Sun et al., 2023), a semi-structured pruning method yielding sparse models not suitable for most hardware. Compared to LLM-Pruner (Ma et al., 2023) and Bonsai (Dery et al., 2024), our model achieves (over 1.2 \times) higher inference speedup with significantly better performance (11.8 vs 19.24 perplexity). Pruning takes only 2 hours on a single GPU, about half the time of Bonsai. Additionally, low-rank weight adaptation (Hu et al., 2021) enables us to fine-tune all modules within the same timeframe. Fine-tuning results are in Appendix B.1. We also test our 50% pruned LLaMA on zero-shot reasoning tasks shown in Table 5. Overall, our pruned model outperforms other techniques with significantly lower prune time.

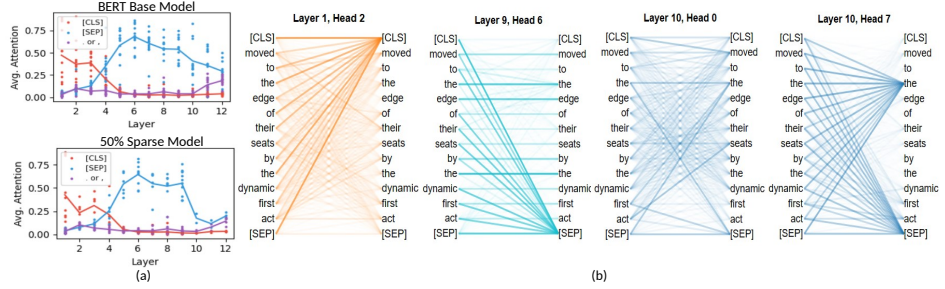


Figure 5: (a) Comparative attention allocation towards special tokens in un-pruned (top) and pruned (bottom) models. Dots represent token attention by heads, with lines indicating mean attention by remaining heads. Pruned model exhibits reduced special token attention (b) Eliminated heads example: those highly attentive to CLS, SEP, current token, common articles like 'the' and displaying broad attention. Line thickness reflects attention weight towards the token.

5.5 Ablation Study

Effect of pruning different structures. To investigate the effect of pruning embedding states unlike other previous state-of-the-art approaches, we conduct ablation studies. On removing the choice to prune the embedding states, as seen in Table 4, the performance decreases across all tasks. This is attributed to the increased pruning of other model structures - the layers, hidden states and the attention heads. On not pruning the layers, the models with higher sparsity levels suffer most in terms of speedup while performance degrades slightly. When both the embeddings and layers are not pruned, the algorithm prunes more attention heads and hidden states leading to lower performance of models at 60% sparsity levels with higher sparsity (95%) levels affected most in terms of both speedup and performance.

Importance of distillation. We analyze the impact of the distillation objectives in conjunction with our VIB-based pruning approach on pruned model performance in Table 6. We note that ablating layer-wise knowledge distillation from dynamically matched teacher layers to student layers results in a performance drop of 1 to 3 points. Completely ablating knowledge distillation leads to a performance drop of 2 to 4 points across all datasets. This shows that distillation helps improve the pruning performance of our VIB-based method by retaining performance of the student models during the iterative pruning process.

6 Qualitative Analysis

Computing Average Attention in Heads. We evaluate information preservation and redundancy reduction in pruned models while maintaining performance by analyzing attention heads in both pre-trained BERT and an equivalently performing pruned model. On the SST-2 downstream task, we compare the un-pruned BERT base model with a 50% smaller sized model. Our examination includes computing average attention directed towards special tokens (SEP, CLS, periods, and commas) as done by Clark et al. (2019). In Figure 5(a), we observe significant attention allocation to special tokens in the un-pruned model. Clark et al. (2019) speculate that attention to these tokens might serve as 'no-ops' when a head's function is not applicable, making such heads viable candidates for pruning. In the 50% pruned model, we confirm this observation, noticing a reduction in attention heads in the latter layers (10-12) and a drastic decrease in average attention towards these tokens in the remaining heads. Additionally, we observe a shift in average attention in each layer from

	QNLI		MNLI		SQuAD	
	(60%)	(95%)	(60%)	(95%)	(60%)	(95%)
Our Method	91.5	81.9	84.3	74.2	87.0	79.6
$-\mathcal{L}_{layer}$	90.2	80.4	83.4	73.6	86.5	76.3
$-\mathcal{L}_{pred}, \mathcal{L}_{layer}$	89.8	79.6	82.9	72.4	86.2	75.5

Table 6: Ablation Experiments with and without distillation losses at different model sparsity levels.

the current token to the previous and next token in the pruned model (see Appendix D.3).

Redundancy in Attention Heads. We visualize attention heads¹ to identify redundant and preserved language aspects in pruned models. In Figure 5(b) displaying attention weights, we observe that heads with high focus on CLS or SEP tokens and excessive attention to the current token are often pruned. Similarly, heads with broad attention or a focus on common articles like ‘the’ or ‘a’ are removed. Moreover, we observe that our method aligns with the interpretation by Burgess et al. (2018) suggesting that VIB encourages the acquisition of more disentangled representations (see Appendix D.4).

7 Conclusion

Integrating the Variational Information Bottleneck principle, our structured pruning method efficiently prunes redundant units across all structural levels in transformers. This results in upto 70% higher compression compared to prior methods, accompanied by minimal accuracy loss (<1%) on GLUE and SQuAD tasks, along with up to 4x inference speedup. Unlike previous approaches, we address both parameter and FLOPs constraints with our task-specific distillation approach, requiring significantly lower training resources (upto 60x less) than task-agnostic methods while achieving similar performance. Our efficient compression variants, namely *Fast* and *Faster-VTrans*, deliver over 10x pruning-speedup with performance comparable to previous state-of-the-art approaches. Our evaluation encompasses various architectures, including decoder-based GPT models. Demonstrating the effectiveness and scalability of our method, we compress the large LLaMA-2 model by 50% with better performance (7 points) and enhanced inference speed (1.2 \times) than other structured pruning methods with lower compression time. Our qualitative analysis supports the competitiveness of our approach, with potential for further quantification in future work.

References

Gustavo Aguilera, Yuan Ling, Yu Zhang, Benjamin Yao, Xing Fan, and Chenlei Guo. Knowledge distillation from internal representations. In *Proceedings of the AAAI Conference on Artificial Intelligence*, volume 34, pp. 7350–7357, 2020.

Alexander A Alemi, Ian Fischer, Joshua V Dillon, and Kevin Murphy. Deep variational information bottleneck. *arXiv preprint arXiv:1612.00410*, 2016.

Haoli Bai, Wei Zhang, Lu Hou, Lifeng Shang, Jing Jin, Xin Jiang, Qun Liu, Michael Lyu, and Irwin King. Binarybert: Pushing the limit of bert quantization, 2021.

Roy Bar-Haim, Ido Dagan, Bill Dolan, Lisa Ferro, and Danilo Giampiccolo. The second pascal recognising textual entailment challenge. *Proceedings of the Second PASCAL Challenges Workshop on Recognising Textual Entailment*, 01 2006.

Luisa Bentivogli, Bernardo Magnini, Ido Dagan, Hoa Trang Dang, and Danilo Giampiccolo. The fifth PASCAL recognizing textual entailment challenge. In *Proceedings of the Second Text Analysis Conference, TAC 2009, Gaithersburg, Maryland, USA, November 16–17, 2009*. NIST, 2009. URL https://tac.nist.gov/publications/2009/additional.papers/RTE5_overview.proceedings.pdf.

Tom Brown, Benjamin Mann, Nick Ryder, Melanie Subbiah, Jared D Kaplan, Prafulla Dhariwal, Arvind Neelakantan, Pranav Shyam, Girish Sastry, Amanda Askell, et al. Language models are few-shot learners. *Advances in neural information processing systems*, 33:1877–1901, 2020.

Christopher P Burgess, Irina Higgins, Arka Pal, Loic Matthey, Nick Watters, Guillaume Desjardins, and Alexander Lerchner. Understanding disentangling in \beta-vae. *arXiv preprint arXiv:1804.03599*, 2018.

¹<https://github.com/jessevig/bertviz>

Daniel Cer, Mona Diab, Eneko Agirre, Iñigo Lopez-Gazpio, and Lucia Specia. SemEval-2017 task 1: Semantic textual similarity multilingual and crosslingual focused evaluation. In *Proceedings of the 11th International Workshop on Semantic Evaluation (SemEval-2017)*, pp. 1–14, Vancouver, Canada, August 2017. Association for Computational Linguistics. doi: 10.18653/v1/S17-2001. URL <https://aclanthology.org/S17-2001>.

Cheng Chen, Yichun Yin, Lifeng Shang, Zhi Wang, Xin Jiang, Xiao Chen, and Qun Liu. Extract then distill: Efficient and effective task-agnostic bert distillation, 2021.

Kevin Clark, Urvashi Khandelwal, Omer Levy, and Christopher D. Manning. What does BERT look at? an analysis of BERT’s attention. In *Proceedings of the 2019 ACL Workshop BlackboxNLP: Analyzing and Interpreting Neural Networks for NLP*, pp. 276–286, Florence, Italy, August 2019. Association for Computational Linguistics. doi: 10.18653/v1/W19-4828. URL <https://aclanthology.org/W19-4828>.

Ido Dagan, Oren Glickman, and Bernardo Magnini. The pascal recognising textual entailment challenge. In Joaquin Quiñonero-Candela, Ido Dagan, Bernardo Magnini, and Florence d’Alché Buc (eds.), *Machine Learning Challenges. Evaluating Predictive Uncertainty, Visual Object Classification, and Recognising Tectual Entailment*, pp. 177–190, Berlin, Heidelberg, 2006. Springer Berlin Heidelberg. ISBN 978-3-540-33428-6.

Bin Dai, Chen Zhu, Baining Guo, and David Wipf. Compressing neural networks using the variational information bottleneck. In *International Conference on Machine Learning*, pp. 1135–1144. PMLR, 2018.

Lucio Dery, Steven Kolawole, Jean-Francois Kagey, Virginia Smith, Graham Neubig, and Ameet Talwalkar. Everybody prune now: Structured pruning of llms with only forward passes. *arXiv preprint arXiv:2402.05406*, 2024.

William B. Dolan and Chris Brockett. Automatically constructing a corpus of sentential paraphrases. In *Proceedings of the Third International Workshop on Paraphrasing (IWP2005)*, 2005. URL <https://aclanthology.org/I05-5002>.

Oshin Dutta, Tanu Kanvar, and Sumeet Agarwal. Search-time efficient device constraints-aware neural architecture search. *arXiv preprint arXiv:2307.04443*, 2023.

Angela Fan, Edouard Grave, and Armand Joulin. Reducing transformer depth on demand with structured dropout. In *International Conference on Learning Representations*, 2020. URL <https://openreview.net/forum?id=Syl02yStDr>.

Elias Frantar and Dan Alistarh. Sparsegpt: Massive language models can be accurately pruned in one-shot. In *International Conference on Machine Learning*, pp. 10323–10337. PMLR, 2023.

Danilo Giampiccolo, Bernardo Magnini, Ido Dagan, and Bill Dolan. The third PASCAL recognizing textual entailment challenge. In *Proceedings of the ACL-PASCAL Workshop on Textual Entailment and Paraphrasing*, pp. 1–9, Prague, June 2007. Association for Computational Linguistics. URL <https://aclanthology.org/W07-1401>.

Song Han, Jeff Pool, John Tran, and William Dally. Learning both weights and connections for efficient neural network. In C. Cortes, N. Lawrence, D. Lee, M. Sugiyama, and R. Garnett (eds.), *Advances in Neural Information Processing Systems*, volume 28. Curran Associates, Inc., 2015. URL https://proceedings.neurips.cc/paper_files/paper/2015/file/ae0eb3eed39d2bcef4622b2499a05fe6-Paper.pdf.

James Henderson and Fabio Fehr. A variational autoencoder for transformers with nonparametric variational information bottleneck. *arXiv preprint arXiv:2207.13529*, 2022.

Geoffrey Hinton, Oriol Vinyals, and Jeff Dean. Distilling the knowledge in a neural network, 2015.

Lu Hou, Zhiqi Huang, Lifeng Shang, Xin Jiang, Xiao Chen, and Qun Liu. Dynabert: Dynamic bert with adaptive width and depth. In H. Larochelle, M. Ranzato, R. Hadsell, M.F. Balcan, and H. Lin (eds.), *Advances in Neural Information Processing Systems*, volume 33, pp. 9782–9793. Curran Associates, Inc., 2020. URL https://proceedings.neurips.cc/paper_files/paper/2020/file/6f5216f8d89b086c18298e043bfe48ed-Paper.pdf.

E Hu, Y Shen, P Wallis, Z Allen-Zhu, Y Li, S Wang, L Wang, and W Chen. Low-rank adaptation of large language models. *arXiv*, 2021.

Kun Huang, Xin Guo, and Meng Wang. Towards efficient pre-trained language model via feature correlation distillation. In *Thirty-seventh Conference on Neural Information Processing Systems*, 2023.

Xiaoqi Jiao, Yichun Yin, Lifeng Shang, Xin Jiang, Xiao Chen, Linlin Li, Fang Wang, and Qun Liu. Tinybert: Distilling bert for natural language understanding. *arXiv preprint arXiv:1909.10351*, 2019.

Simran Khanuja, Melvin Johnson, and Partha Talukdar. MergeDistill: Merging language models using pre-trained distillation. In *Findings of the Association for Computational Linguistics: ACL-IJCNLP 2021*, pp. 2874–2887, Online, August 2021. Association for Computational Linguistics. doi: 10.18653/v1/2021.findings-acl.254. URL <https://aclanthology.org/2021.findings-acl.254>.

Sehoon Kim, Amir Gholami, Zhewei Yao, Michael W Mahoney, and Kurt Keutzer. I-bert: Integer-only bert quantization. *International Conference on Machine Learning (Accepted)*, 2021.

Joseph B Kruskal. Multidimensional scaling by optimizing goodness of fit to a nonmetric hypothesis. *Psychometrika*, 29(1):1–27, 1964.

Woosuk Kwon, Sehoon Kim, Michael W. Mahoney, Joseph Hassoun, Kurt Keutzer, and Amir Gholami. A Fast Post-Training Pruning Framework for Transformers, October 2022. URL <http://arxiv.org/abs/2204.09656>. arXiv:2204.09656 [cs].

François Lagunas, Ella Charlaix, Victor Sanh, and Alexander Rush. Block pruning for faster transformers. In *Proceedings of the 2021 Conference on Empirical Methods in Natural Language Processing*, pp. 10619–10629, Online and Punta Cana, Dominican Republic, November 2021. Association for Computational Linguistics. doi: 10.18653/v1/2021.emnlp-main.829. URL <https://aclanthology.org/2021.emnlp-main.829>.

Yixiao Li, Yifan Yu, Qingru Zhang, Chen Liang, Pengcheng He, Weizhu Chen, and Tuo Zhao. Losparse: Structured compression of large language models based on low-rank and sparse approximation. *arXiv preprint arXiv:2306.11222*, 2023.

Chen Liang, Simiao Zuo, Minshuo Chen, Haoming Jiang, Xiaodong Liu, Pengcheng He, Tuo Zhao, and Weizhu Chen. Super tickets in pre-trained language models: From model compression to improving generalization, 2021.

Chen Liang, Haoming Jiang, Zheng Li, Xianfeng Tang, Bin Yin, and Tuo Zhao. HomoDistil: Homotopic Task-Agnostic Distillation of Pre-trained Transformers, February 2023a. URL <http://arxiv.org/abs/2302.09632>. arXiv:2302.09632 [cs].

Chen Liang, Simiao Zuo, Qingru Zhang, Pengcheng He, Weizhu Chen, and Tuo Zhao. Less is more: Task-aware layer-wise distillation for language model compression. In *International Conference on Machine Learning*, pp. 20852–20867. PMLR, 2023b.

Xinyin Ma, Gongfan Fang, and Xinchao Wang. Llm-pruner: On the structural pruning of large language models. *arXiv preprint arXiv:2305.11627*, 2023.

J. S. McCarley, Rishav Chakravarti, and Avirup Sil. Structured pruning of a bert-based question answering model, 2021.

Stephen Merity, Caiming Xiong, James Bradbury, and Richard Socher. Pointer sentinel mixture models. *arXiv preprint arXiv:1609.07843*, 2016.

Paul Michel, Omer Levy, and Graham Neubig. Are sixteen heads really better than one? In H. Wallach, H. Larochelle, A. Beygelzimer, F. d'Alché-Buc, E. Fox, and R. Garnett (eds.), *Advances in Neural Information Processing Systems*, volume 32. Curran Associates, Inc., 2019. URL https://proceedings.neurips.cc/paper_files/paper/2019/file/2c601ad9d2ff9bc8b282670cdd54f69f-Paper.pdf.

Anshul Nasery, Hardik Shah, Arun Sai Suggala, and Prateek Jain. End-to-end neural network compression via $\frac{\ell_1}{\ell_2}$ regularized latency surrogates. *arXiv preprint arXiv:2306.05785*, 2023.

Colin Raffel, Noam Shazeer, Adam Roberts, Katherine Lee, Sharan Narang, Michael Matena, Yanqi Zhou, Wei Li, and Peter J Liu. Exploring the limits of transfer learning with a unified text-to-text transformer. *The Journal of Machine Learning Research*, 21(1):5485–5551, 2020.

Pranav Rajpurkar, Jian Zhang, Konstantin Lopyrev, and Percy Liang. Squad: 100,000+ questions for machine comprehension of text, 2016.

Alex Renda, Jonathan Frankle, and Michael Carbin. Comparing rewinding and fine-tuning in neural network pruning, 2020.

Adriana Romero, Nicolas Ballas, Samira Ebrahimi Kahou, Antoine Chassang, Carlo Gatta, and Yoshua Bengio. Fitnets: Hints for thin deep nets, 2015.

Hassan Sajjad, Fahim Dalvi, Nadir Durrani, and Preslav Nakov. Poor man's bert: Smaller and faster transformer models. *ArXiv*, abs/2004.03844, 2020.

Victor Sanh, Lysandre Debut, Julien Chaumond, and Thomas Wolf. Distilbert, a distilled version of bert: smaller, faster, cheaper and lighter, 2020a.

Victor Sanh, Thomas Wolf, and Alexander Rush. Movement pruning: Adaptive sparsity by fine-tuning. In H. Larochelle, M. Ranzato, R. Hadsell, M.F. Balcan, and H. Lin (eds.), *Advances in Neural Information Processing Systems*, volume 33, pp. 20378–20389. Curran Associates, Inc., 2020b. URL https://proceedings.neurips.cc/paper_files/paper/2020/file/eae15aabaa768ae4a5993a8a4f4fa6e4-Paper.pdf.

Noam Slonim and Naftali Tishby. Agglomerative information bottleneck. In S. Solla, T. Leen, and K. Müller (eds.), *Advances in Neural Information Processing Systems*, volume 12. MIT Press, 1999. URL https://proceedings.neurips.cc/paper_files/paper/1999/file/be3e9d3f7d70537357c67bb3f4086846-Paper.pdf.

Richard Socher, Alex Perelygin, Jean Wu, Jason Chuang, Christopher D. Manning, Andrew Ng, and Christopher Potts. Recursive deep models for semantic compositionality over a sentiment treebank. In *Proceedings of the 2013 Conference on Empirical Methods in Natural Language Processing*, pp. 1631–1642, Seattle, Washington, USA, October 2013. Association for Computational Linguistics. URL <https://aclanthology.org/D13-1170>.

Ayush Srivastava, Oshin Dutta, Jigyasa Gupta, Sumeet Agarwal, and Prathosh AP. A variational information bottleneck based method to compress sequential networks for human action recognition. In *Proceedings of the IEEE/CVF Winter Conference on Applications of Computer Vision*, pp. 2745–2754, 2021.

Mingjie Sun, Zhuang Liu, Anna Bair, and J Zico Kolter. A simple and effective pruning approach for large language models. *arXiv preprint arXiv:2306.11695*, 2023.

S. Sun, Yu Cheng, Zhe Gan, and Jingjing Liu. Patient knowledge distillation for bert model compression. In *Conference on Empirical Methods in Natural Language Processing*, 2019.

Zhiqing Sun, Hongkun Yu, Xiaodan Song, Renjie Liu, Yiming Yang, and Denny Zhou. MobileBERT: a Compact Task-Agnostic BERT for Resource-Limited Devices. In *Proceedings of the 58th Annual Meeting of the Association for Computational Linguistics*, pp. 2158–2170, Online, July 2020. Association for Computational Linguistics. doi: 10.18653/v1/2020.acl-main.195. URL <https://aclanthology.org/2020.acl-main.195>.

Raphael Tang, Yao Lu, Linqing Liu, Lili Mou, Olga Vechtomova, and Jimmy Lin. Distilling task-specific knowledge from bert into simple neural networks, 2019.

Naftali Tishby and Noga Zaslavsky. Deep learning and the information bottleneck principle. In *2015 IEEE Information Theory Workshop (ITW)*, pp. 1–5. IEEE, 2015.

Hugo Touvron, Thibaut Lavril, Gautier Izacard, Xavier Martinet, Marie-Anne Lachaux, Timothée Lacroix, Baptiste Rozière, Naman Goyal, Eric Hambro, Faisal Azhar, Aurelien Rodriguez, Armand Joulin, Edouard Grave, and Guillaume Lample. Llama: Open and efficient foundation language models, 2023.

Iulia Turc, Ming-Wei Chang, Kenton Lee, and Kristina Toutanova. Well-read students learn better: On the importance of pre-training compact models, 2019.

Ashish Vaswani, Noam Shazeer, Niki Parmar, Jakob Uszkoreit, Llion Jones, Aidan N Gomez, Łukasz Kaiser, and Illia Polosukhin. Attention is all you need. In I. Guyon, U. Von Luxburg, S. Bengio, H. Wallach, R. Fergus, S. Vishwanathan, and R. Garnett (eds.), *Advances in Neural Information Processing Systems*, volume 30. Curran Associates, Inc., 2017. URL https://proceedings.neurips.cc/paper_files/paper/2017/file/3f5ee243547dee91fdb053c1c4a845aa-Paper.pdf.

Elena Voita, David Talbot, Fedor Moiseev, Rico Sennrich, and Ivan Titov. Analyzing Multi-Head Self-Attention: Specialized Heads Do the Heavy Lifting, the Rest Can Be Pruned, June 2019. URL <http://arxiv.org/abs/1905.09418>. arXiv:1905.09418 [cs].

Alex Wang, Amanpreet Singh, Julian Michael, Felix Hill, Omer Levy, and Samuel Bowman. GLUE: A multi-task benchmark and analysis platform for natural language understanding. In *Proceedings of the 2018 EMNLP Workshop BlackboxNLP: Analyzing and Interpreting Neural Networks for NLP*, pp. 353–355, Brussels, Belgium, November 2018. Association for Computational Linguistics. doi: 10.18653/v1/W18-5446. URL <https://aclanthology.org/W18-5446>.

Wenhui Wang, Hangbo Bao, Shaohan Huang, Li Dong, and Furu Wei. Minilmv2: Multi-head self-attention relation distillation for compressing pretrained transformers. *arXiv preprint arXiv:2012.15828*, 2020a.

Wenhui Wang, Furu Wei, Li Dong, Hangbo Bao, Nan Yang, and Ming Zhou. Minilm: Deep self-attention distillation for task-agnostic compression of pre-trained transformers. *Advances in Neural Information Processing Systems*, 33:5776–5788, 2020b.

Ziheng Wang, Jeremy Wohlwend, and Tao Lei. Structured Pruning of Large Language Models. In *Proceedings of the 2020 Conference on Empirical Methods in Natural Language Processing (EMNLP)*, pp. 6151–6162, 2020c. doi: 10.18653/v1/2020.emnlp-main.496. URL <http://arxiv.org/abs/1910.04732>. arXiv:1910.04732 [cs, stat].

Alex Warstadt, Amanpreet Singh, and Samuel R. Bowman. Neural network acceptability judgments. *Transactions of the Association for Computational Linguistics*, 7:625–641, 2019. doi: 10.1162/tacl_a_00290. URL <https://aclanthology.org/Q19-1040>.

Adina Williams, Nikita Nangia, and Samuel Bowman. A broad-coverage challenge corpus for sentence understanding through inference. In *Proceedings of the 2018 Conference of the North American Chapter of the Association for Computational Linguistics: Human Language Technologies, Volume 1 (Long Papers)*, pp. 1112–1122. Association for Computational Linguistics, 2018. URL <http://aclweb.org/anthology/N18-1101>.

Mengzhou Xia, Zexuan Zhong, and Danqi Chen. Structured pruning learns compact and accurate models. In *Association for Computational Linguistics (ACL)*, 2022.

Nakyeong Yang, Yunah Jang, Hwanhee Lee, Seohyeong Jung, and Kyomin Jung. Task-specific compression for multi-task language models using attribution-based pruning. *arXiv preprint arXiv:2205.04157*, 2022.

Ofir Zafrir, Guy Boudoukh, Peter Izsak, and Moshe Wasserblat. Q8bert: Quantized 8bit bert. In *2019 Fifth Workshop on Energy Efficient Machine Learning and Cognitive Computing - NeurIPS Edition (EMC2-NIPS)*. IEEE, December 2019. doi: 10.1109/emc2-nips53020.2019.00016. URL <http://dx.doi.org/10.1109/EMC2-NIPS53020.2019.00016>.

Ofir Zafrir, Ariel Larey, Guy Boudoukh, Haihao Shen, and Moshe Wasserblat. Prune once for all: Sparse pre-trained language models, 2021.

Michael Zhu and Suyog Gupta. To prune, or not to prune: exploring the efficacy of pruning for model compression, 2017.

Algorithm 1 Our primary method variant - Identifying redundant units with VIB-based masks with user-defined parameters or FLOPs constraint

Input: Pruning metric (parameters or FLOPs), target metric t , Teacher Model

Initialize: VIB masks $z_m, z_a, z_{out}, z_{layer}$

for $e = 1, \dots, Epochs$ **do**

 Calculate VIB loss $\tilde{\mathcal{L}}_{VIB}$

 Calculate expected sparsity s_e

 Calculate sparsity loss \mathcal{L}_s

 Total loss $\mathcal{L}_{total} = \mathcal{L}_{distil} + \tilde{\mathcal{L}}_{VIB} + \mathcal{L}_s$

 Update model $f(\cdot; \theta_s)$ weights θ_s

 Update z masks

 Update λ_1, λ_2

end for

Convert z masks to binary masks $\hat{z}_{i,j}^{mask}$

Fine-tune VIB mask-selected model weights by minimizing $\mathcal{L}_{total} = \mathcal{L}_{distil} + \tilde{\mathcal{L}}_{VIB}$

Prune VIB mask-selected units from model

$\hat{f}(\cdot; \theta_s) \leftarrow f(\cdot; \theta_s) \odot \hat{z}_{i,j}^{mask}$

Output: Compressed model $\hat{f}(\cdot; \theta_s)$

Method	Pruning Setting	Pruning Granularity	Distillation Setting	Student Initialization
DistiBERT (Sanh et al., 2020a)	no pruning	-	TA	Un-trained weights
TinyBERT-GD (Jiao et al., 2019)	no pruning	-	TA	Un-trained weights
MiniLM (Wang et al., 2020b)	no pruning	-	TA	Un-trained weights
HomoDistil (Liang et al., 2023a)	prune while distill	Row, Column	TA	pre-trained weights
DynaBERT (Hou et al., 2020)	prune, then distill	FFN, Head	TS	Pruned, Pre-trained weights
Block Pruning (Lagunas et al., 2021)	prune, then distill	weight blocks	TS	Pruned, Pre-trained weights
Post-prune (Kwon et al., 2022)	prune	MHA, FFN	none	-
CoFiXia (Xia et al., 2022)	prune while distill	Head, FFN, Layers	TS	Pre-trained weights
Our method	prune while distill	Embeddings, Head, FFN, Layers	TA/TS	Pre-trained/finetuned teacher weights
SparseGPT (Frantar & Alistarh, 2023)	prune	MHA, FFN	none	-
Wanda (Sun et al., 2023)	prune	MHA, FFN	none	-
LLM-Pruner (Ma et al., 2023)	prune	MHA, FFN	none	-
Bonsai (Dery et al., 2024)	prune	MHA, FFN	TS	Pre-trained compressed model
Our method (for LLM pruning)	prune	Embeddings, Head, FFN, Layers	TS	Pre-trained compressed model

Table 7: Comparison of the baseline methods with our method in terms of pruning and distillation techniques. TS - indicates task specific; TA - Task agnostic distillation

A Further Training details

A.1 Datasets

General Language Understanding Evaluation (GLUE) (Wang et al., 2018) is a collection of nine natural language understanding tasks. The GLUE tasks encompass various domains, including sentiment analysis (SST2, (Socher et al., 2013)), natural language inference (MNLI, (Williams et al., 2018)), paraphrase identification (QQP and QNLI), textual entailment (MRPC, (Dolan & Brockett, 2005)), linguistic acceptability (CoLA (Warstadt et al., 2019)), semantic textual similarity (STS-B (Cer et al., 2017)), and recognizing textual entailment (RTE (Dagan et al., 2006; Bar-Haim et al., 2006; Giampiccolo et al., 2007; Bentivogli et al., 2009)).

Stanford Question Answering Dataset (SQuAD) (Rajpurkar et al., 2016) is a reading comprehension dataset, consisting of questions posed on Wikipedia articles, where the answer are a segment of the comprehension text.

WikiText-2 Created from Wikipedia articles Merity et al. (2016), this dataset consists of 2 million tokens for training and more than 200,000 tokens in the validation and test set.

A.2 Further details about the baseline models

In Table 7, we present a comprehensive comparative analysis of the various baseline methods used for performance evaluation in Section 5.

DistilBERT (Sanh et al., 2020a) employs a vanilla distillation approach during the pre-training phase by considering the distillation loss over the outputs of the models. **TinyBERT** (Jiao et al., 2019) builds upon DistilBERT by leveraging knowledge from intermediate Transformer layers. **MiniLM** (Wang et al., 2020b) targets the discrepancy between queries-keys scaled dot product and values-values scaled dot product in the final layer’s self-attention module. Extending on MiniLM, MiniLMv2 (Wang et al., 2020a) emphasizes on the emulation of attention head relations from the teacher model. Employing a task-agnostic distillation approach, **HomoDistil** (Liang et al., 2023a) distils knowledge into iteratively pruned students initialized to the teacher’s weights. **DynaBERT** (Hou et al., 2020) offers flexibility to adjust the model size and latency by selecting an adaptive width and depth. The training involves an initial training of a width-adaptive model followed by enabling adaptability in both width and depth, using distillation from the full-size model. **CoFi** (Xia et al., 2022) adopts an iterative pruning strategy during the finetuning phase, utilizing distillation from the larger task-specific teacher models to the student. It performs simultaneously pruning of attention heads, FFNs and whole layers. Movement Pruning (Sanh et al., 2020b) proposes a deterministic first-order weight pruning method, that is effective in finetuning regime of pre-trained models. **BlockPruning** Lagunas et al. (2021) uses this method to prune blocks of weight matrices, allowing for better optimizations on dense hardware. **Post-Prune** uses post-training pruning framework (Aguilar et al., 2020) that proposes a Fisher-based technique to train masks for identification of redundant neurons and selectively fine-tunes only the masks to specific tasks.

We show the scaling ability of our pruning technique to prune large language models like LLaMA-2 (Touvron et al., 2023). Comparison with previous techniques includes **SparseGPT** (Frantar & Alistarh, 2023) which proposes a second-order layer-wise pruning method that approximates closed form equations thus being able to scale up pruning LLMs. **Wanda** (Sun et al., 2023) takes into account the norm of weights and input activations for pruning weights in an unstructured/structured manner. **Bonsai** (Dery et al., 2024) is a gradient-free structured pruning method that estimates module importance perturbatively by generating sub-models and evaluating their performances. **LLM-pruner** (Ma et al., 2023) is a structured pruning method that uses gradient information to prune large language models in a task-agnostic manner.

A.3 Influence of Dataset size on pruning and finetuning time

We prune with different number of samples from the datasets within GLUE with our *Fast-VTrans* method as seen in Figure 6. For both the faster variants, we use 8000 samples from large datasets (MNLI, QNLI, QQP, SST-2, SQuAD) and 2000 samples from the small datasets (MRPC, RTE, STSB, CoLA) during pruning. Further increasing the samples leads to a 2x to 4x increase in prune time with only about 1% boost in performance. During finetuning with the faster variants, we use 16000 samples for large datasets and the whole small datasets.

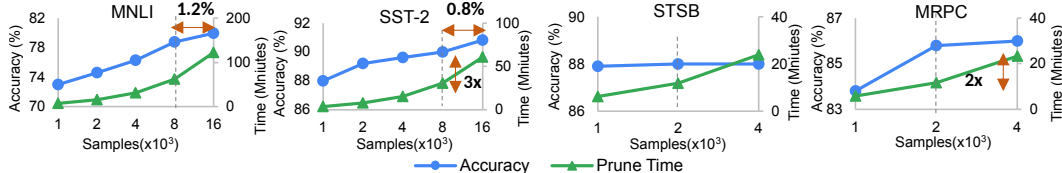


Figure 6: Data subset impact: Prune time rises exponentially with data samples, while model performance stabilizes.

Hyper-parameters	GLUE(small)	GLUE(large)	SQuAD
VIB learning rate	$\{1 \text{ to } 2\} \times 10^{-2}$	$\{1 \text{ to } 2\} \times 10^{-2}$	$\{1 \text{ to } 2\} \times 10^{-3}$
Training Learning Rate	$\{2\} \times 10^{-5}$	$\{2\} \times 10^{-5}$	$\{3\} \times 10^{-5}$
Fine-tuning Learning Rate	$\{2 \text{ to } 7\} \times 10^{-5}$	$\{2 \text{ to } 7\} \times 10^{-5}$	$\{2 \text{ to } 7\} \times 10^{-5}$
Batch Size	32	32	16
Fine-tune Epochs	20	10	3
Distillation η	0.5	0.5	0.5

Table 8: Hyper-parameter configurations for pruning and finetuning with our method and its variants on GLUE and SQuAD datasets. Experiments are conducted on NVIDIA V100 GPU.

VIB LR	Dataset size	block_size	weights LR	LoRA-rank	LoRA- α	η (distill Weight)	block_size
5×10^{-2}	4000	512	1×10^{-4}	128	$4 \times \text{rank}$	0.01	512

(a)

(b)

Table 9: Hyper-parameters for (a) pruning with Faster-VTrans and (b) for fine-tuning compressed model on WikiText-2 Dataset

A.4 Influence of number of epochs

The number of epochs used to finetune the model is varied from 5 to 20 as seen in Figure 7. For smaller GLUE tasks, we finetune the weights of the student model with distillation for 20 epochs. For larger GLUE tasks, we finetune for 10 epochs with distillation. Increasing the number of epochs for larger datasets (MNLI, SST-2) is seen to increase the time by 2x with less than 1% increase in accuracy.

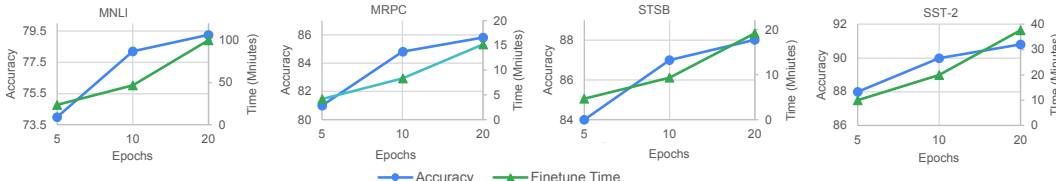


Figure 7: We finetune the models obtained with sparsity of 75% with different number of epochs and evaluate the final performance.

A.5 Implementation Details of experiments with GLUE and SQuAD

We list the hyper-parameter setting for task-specific pruning and finetuning with our method on GLUE and SQuAD tasks in Table 8. Experiments are performed on a single NVIDIA V100 GPU (32GB). In task-specific setting, we finetune the pre-trained BERT-base to particular tasks for 3 (large datasets) and 10 (small datasets) epochs to obtain teachers as used in previously [Hou et al. \(2020\)](#). BERT model previously finetuned on MNLI task is utilized to get teachers of smaller GLUE datasets - RTE, MRPC and STS-B. These teacher yield high performing models.

For *VTrans* and *Fast-VTrans*: We prune and finetune with our objective function for 20 epochs to obtain smaller student models within the given sparsity constraint. Epochs lower than 20 does not let the pruning algorithm converge for higher sparsity levels ($\geq 80\%$). For lower sparsity levels, the algorithm converges within less than 10 epochs. For *Faster-VTrans*, we freeze the model parameters while training only the VIB masks.

For our task-agnostic variant, we use similar hyperparameters used by [Jiao et al. \(2019\)](#) and VIB parameters are kept as in Table 8. We use 8 NVIDIA V100 to prune the BERT-base pre-trained model for 3 epochs. The pruned model is finetuned for 20 epochs on small and 10 the large tasks of GLUE and SQuAD as seen optimal in Figure 7.

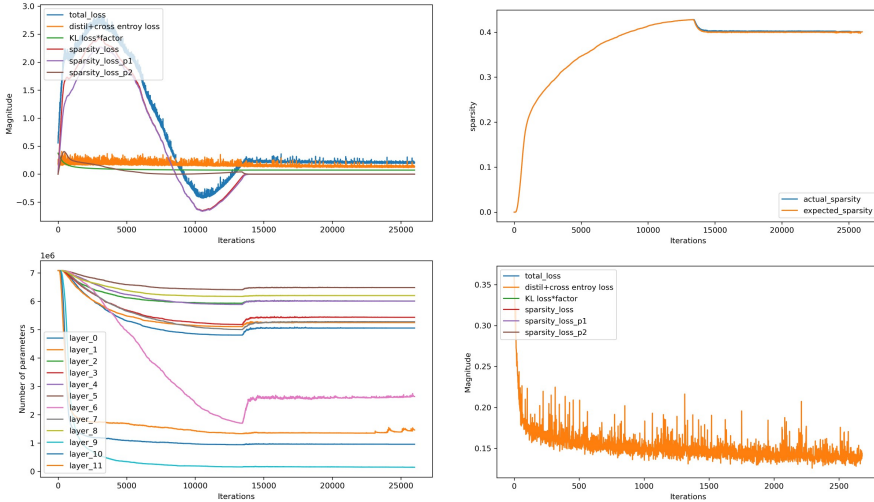


Figure 8: Training plots for the CoLA dataset under a 40% model size sparsity constraint. Top left: illustrates the evolution of various loss objectives over training iterations. Top right: the pruning trajectory stabilizes with increasing iterations. Bottom left: depicts the trajectory of remaining parameters in each layer. Bottom right: showcases different loss trajectories during finetuning.

A.6 Implementation details with experiments on WikiText-2

Our pruning method *Faster-VTrans* essentially only introduces a single hyper-parameter, the VIB learning rate, which we set at 5×10^{-2} . Increasing the VIB learning rate (LR) reduces pruning time but may result in lower model performance. Conversely, decreasing the VIB LR improves model performance but requires more data samples to converge to the user-defined sparsity level, thereby increasing pruning time. We prune with only 4000 data samples from the train set to keep our prune time within 2 GPU hours. During finetuning, we use LoRA to finetune the all modules except embeddings. The hyper-parameters are listed in Table 9b. All experiments with LLaMA are run on NVIDIA A6000 GPU (48GB).

A.7 Resources required for pruning LLMs

The details about the number of data samples and maximum sequence length are provided in Table 10 below. Although Bonsai is a forward-pass-only method, it takes approximately 37 hours to prune 50% of the model parameters. This duration is significantly longer than other forward-pass methods and our method due to Bonsai’s exploration of sub-models and repeated evaluations. Bonsai processes one sample with a sequence length of 4096 in a single pass, whereas our method handles one sample with a maximum sequence length of 512 using a single NVIDIA A6000 (48GB) GPU. In contrast, LLM-Pruner requires two GPUs of 80GB each or four 40GB GPUs, which is four times the GPU memory required by our method.

Method	Wikitext2 PPL(w/o) finetune	Max Memory during pruning	Pruning Samples	Sequence length	Pruning Time	Inference Speedup
LLM-pruner	19.24	154 GB	10	64	1 hr	1.5x
Bonsai	19.47	25 GB	32	4096	37 hrs	1.58x
Ours	11.8	36 GB	5000	512	2 hrs	1.82x

Table 10: Comparison of details of pruning LLaMA-2-7B model using structured pruning methods

Model	Params (million)	Inference Speedup	# FLOPs (non-embedding)
BERT-base	109	1.00 ×	1.00 ×
DistilBERT ₆	66	1.98 ×	0.50 ×
TinyBERT ₆ - GD	66	1.98 ×	0.50 ×
MiniLMv1 ₆	66	1.98 ×	0.50 ×
HomoBERT-base	65	1.30 ×	0.56 ×
BERT-small	28.6	4.77 ×	0.15 ×
CoFi _{5%}	28.4	5.16 ×	0.05 ×
TinyBERT _{3×384} -GD	17.0	7.34 ×	0.06 ×
MiniLMv1 ₃	17.0	7.34 ×	0.06 ×
TinyBERT _{4×312} -GD	14.5	6.28 ×	0.07 ×
HomoBERT-xsmall	15.6	2.51 ×	0.10 ×
HomoBERT-tiny	14.1	2.55 ×	0.09 ×
Ours	14.5	4 ×	0.07 ×

Table 11: We analyze and compare the inference speedup and FLOPs count (excluding embedding) for the baselines and our method, relative to BERT-base.

A.8 Pruning/Training plots

We show the trajectory of different losses and layer parameters in our final objective function during pruning and finetuning for a particular task in Figure 8. Our sparsity constraint is seen to stabilize pruning after certain epochs.

A.9 FLOPs and Speedup

With FLOPs constraint in our objective function instead of model parameters, we calculate the sparsity as the reduction in FLOPs of the model to the original FLOPs. We evaluate our model using the Pytorch Profiler (https://pytorch.org/tutorials/recipes/recipes/profiler_recipe.html) and compare the inference speedup and the FLOPs (excluding the embeddings for consistency with other methods) of the baseline models with a model obtained using our method in Table 11. Although certain methods yield models that have faster inference speed, our model can be compressed more in terms of number of parameters than the others while retaining performance.

B Further comparison with other methods

B.1 Comparison on WikiText-2 after fine-tuning pruned LLMs

The performance of models after finetuning on WikiText-2 is seen in Table 12. The performance of our model is slightly worse since we use the WikiText-2 dataset with **5000** data samples for fine-tuning. Whereas, Bonsai, Wanda use c4 (Raffel et al., 2020) dataset with over **15000** samples for finetuning, thus requiring 3 times more fine-tuning time. Before fine-tuning, the model produced by Wanda 2:4 achieves a speedup over the parent model (1.14×). While the performance gap can be bridged by LoRA finetuning (10.52 → 8.34), the adapted semi-structured model experiences a drastic slowdown (0.75×), since the learned low-rank matrices cannot be merged with the original sparsified ones without reverting back to dense computation. SparseGPT already uses weight updates in its algorithm.

Model	Prune Method	Size	Data samples	PPL	Inference Speedup	Prune Time (GPU hrs)
SparseGPT 2:4	semi-structured	3B	-	10.17	1.24x	0.5
Wanda 2:4 w FT	semi-structured	3B	15000	8.34	0.75x	0.06
Bonsai w FT	structured	3B	15000	8.89	1.58	35
Faster-VTrans w FT	structured	3B	5000	9.47	1.82x	2

Table 12: Performance of models pruned from LLaMA-2-7B evaluated on Wikitext-2 after (w) finetuning (FT).

B.2 Stability of the fastest *Faster-VTrans* variant.

We conduct a comparative assessment between the *Faster-VTrans* variant and an analogous fast pruning technique based on Fisher information (Kwon et al., 2022) across various GLUE tasks, as depicted in Figure 9. The models are generated with different FLOP constraints, resulting in models with reduced FLOPs. Notably, for extreme compression (exceeding 50% FLOPs reduction), our method outperforms the alternative approach, yielding models with superior performance. Furthermore, our approach demonstrates models with 2 to 10% lower variance in performance over 10 different random seed initialization, showcasing enhanced stability, as illustrated in the figure.

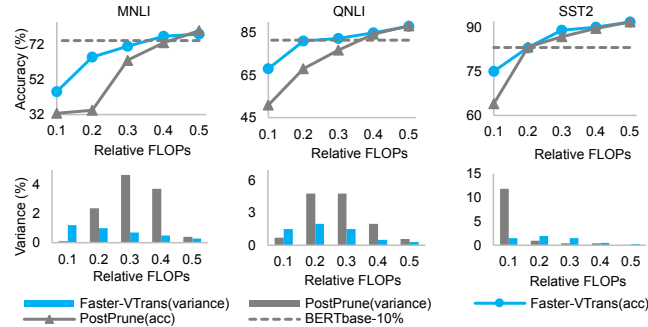


Figure 9: Comparison: *Faster-VTrans* vs. *PostPrune* (Kwon et al., 2022) on 3 GLUE tasks. *Faster-VTrans* achieves superior accuracy and stability on compression from BERT-base

B.3 Pruning BERT-large

We also evaluated our primary approach for compressing large models such as uncased BERT-large. Our models outperform DistilBERT and MINILMv2 on two GLUE tasks while achieving comparable results on the remaining tasks as seen in Table 13.

Model	Parameters (Million)	SST-2 (Acc)	MNLI (Acc)	RTE (Acc)	MRPC (Acc)
BERT _{large}	334	94.9	86.6	83.8	89.3
DistilBERT ₆	66	92.5	82.4	58.4	86.9
MINILMv2 ₆	66	92.4	83.4	71.3	88.6
VTrans	66*	92.5	83.1	73.6	89.1

Table 13: Compression of BERT-large model: Comparing performance of compressed models on GLUE dataset. * indicates the average number of parameters across all datasets.

B.4 Key differences from other iterative pruning methods

We provide a detailed discussion of the key differences of our method from other pruning methods like HomoDistil (Liang et al., 2023a) and CoFi (Xia et al., 2022):

Flexibility in pruning and distillation settings: In Table 7 presents a comprehensive comparison of our method with other baseline techniques concerning pruning and distillation. Notably, our training method exhibits flexibility in working within both task-agnostic and task-specific settings. While HOMODISTIL operates primarily in a specific setting, our approach accommodates both. Moreover, our task-specific setting demonstrates remarkable efficiency with significantly lower resource requirements, utilizing just 1 GPU for tasks such as GLUE and SQuAD, as opposed to the substantial resource demand of at least 8 GPUs and extensive training time in the broader setting.

Performance and Resource Efficiency: Table 3 showcases that our task-specific variant achieves either better or comparable performance in certain tasks compared to HOMODISTIL, despite utilizing fewer GPUs. This efficiency is crucial, demonstrating improved performance with reduced resource demands.

Flexibility in Pruning and Layer Adaptability: Our task-specific pruning methodology, as depicted in Figure 1 identifies varying optimal numbers of embedding states for different tasks. This adaptability is absent in HOMODISTIL, which operates under a task-agnostic paradigm. Furthermore, our embedding masks, FFN layer masks enable flexibility in pruning of layers enabling higher pruning in certain layers - an aspect not accommodated by HOMODISTIL, which maintains consistent layer sizes across all layers.

Metric Constraints : Our method has been tested using both parameters and FLOPs constraints, recognizing that each constraint affects computational operations differently. We emphasize that a lower number of layers is often preferred for inference speedup, while hardware limitations, especially in edge devices like Raspberry Pi, typically align with FLOPs constraints. In contrast, HOMODISTIL manages local sparsity within each layer, focusing on controlling total model parameters.

Explainability and VIB-based Approach: Through our VIB-based method, our approach offers explainability by identifying and pruning redundant units such as attention heads. This feature distinguishes our methodology from HOMODISTIL, which does not explicitly provide explainability for its pruning decisions.

C Further Ablation Experiments on GLUE dataset with BERT

C.1 How many heads are enough without losing accuracy?

On pruning just the attention heads in each layer of the transformer, we see that most GLUE tasks need less than 40% of the attention heads to retain the performance of the model. As seen in Figure 10, for task SST-2, 30% of the heads seem to be enough to retain the performance of the large teacher model.



Figure 10: When only attention heads are pruned, it is seen that for downstream tasks like SST-2, only 30% of the total heads are sufficient to retain performance.

C.2 Ablating Embedding states pruning

We compare the performance of our pruning method specifically with that of CoFi to gauge the efficiency of our VIB-based pruning method with flexible layer sizes in Table 14. For fairness, we ablate the Embedding states pruning and just prune the other modules of the transformer. The teacher which is also the initial student being pruned is the kept same for both the methods.

Tasks	CoFi	Our Method
SST-2	90.6	91.2
MRPC	82.6	82.8
RTE	64.7	65.3
QNLI	86.1	86.9

Table 14: Results showing efficiency of VIB-based pruning coupled with flexible layer sizes in our method. Both methods prune the same structural components- all components except Embedding parameters of BERT base. All models have about 5 million parameters (excluding embeddings)

C.3 Analysis of total prune time

The total compression time mentioned in Table 2 includes the pruning and finetuning time. The breakdown of the same is given in Table 15.

	Prune	Fine-tune
GLUE-high	23%	78%
SQuAD	20%	80%

Table 15: Breakdown of prune time and finetuning time on pruning BERT-base

D Further Qualitative Analysis

D.1 Pruning pattern

We analyze the pruned model structure obtained with our primary compression method. Figure 11 shows the remaining attention heads, intermediate dimensions and hidden states in FFN layers at three different sparsity levels(60%, 70% and 90%) averaged on five datasets within GLUE. From the left-most plot in Figure 11, we note that the over-parameterized embedding layer can be compressed such that 20% of the total embedding states are enough to retain performance of the un-pruned model. We also observe from the other plots in the figure that there is a significant decrease in the intermediate dimensions at all sparsity levels. At higher sparsity levels (at 90%), the latter intermediate and FFN layers are deemed redundant and eliminated. Most of the pruning happens from the latter layers.

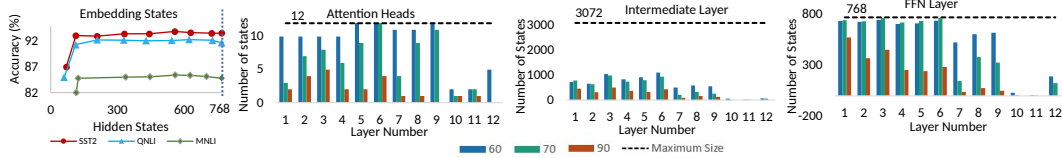


Figure 11: The average pruning pattern across different structural elements of BERT for GLUE tasks. Left plot: Shows pruned models (dots) retain performance at more than 80% lower embedding states.

D.2 More examples of redundant heads

Figure 12 shows more examples of redundant heads with a different input sentence than shown in the main paper. Repetitive heads with attention to CLS tokens, attention to own tokens and broad attention in deemed redundant and can be pruned out from the teacher model.

D.3 Shift of attention to next or previous token

Figure 12 shows how average attention of input tokens in the compressed models change from current token to next or previous token. Attending to current token does not give the model any new information while focusing more on previous or next token might yield better performance.

D.4 Divergent Behavior Among Attention Heads.

We calculate the Jensen-Shannon Divergence $\sum_{\text{token} \in \text{data}} JS(H_i(\text{token}), H_j(\text{token}))$ to measure the pairwise distances between attention head distributions over input data. Using multidimensional scaling [Kruskal \(1964\)](#), we create a two-dimensional representation, ensuring the resulting embeddings closely approximate the Jensen-Shannon distances between

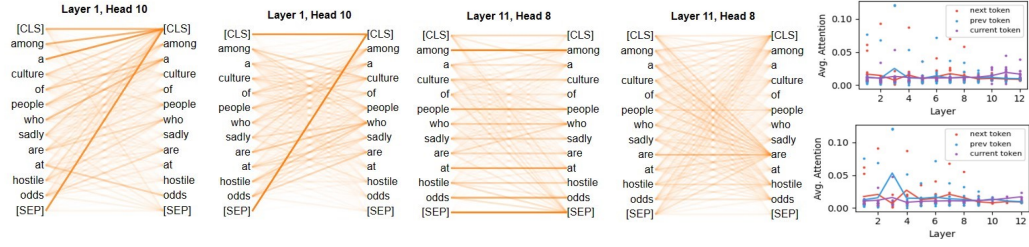


Figure 12: Another example of heads that are deemed redundant and pruned. Repetitive Heads with tokens attending to the CLS token, tokens attending to themselves and heads with broad attention are deemed redundant. Plots show the average attention paid to next, current and previous token in (Top:) Un-pruned model and (Bottom:) pruned model

the corresponding heads. We then visualize the behavior among heads in Figure 13. In the un-pruned BERT model clustering in layers show similar head behavior. Layers 9 to 12 and layers 1 to 4 exhibit close grouping among themselves suggesting analogous behavior in adjacent layers. Conversely, in the pruned model, heads from layers 1 to 4 show a more dispersed distribution, indicating a broader range of behaviors. In the later layers (8 to 11), heads appear sparse and widely dispersed with layer 12 being entirely pruned. This validates our approach, demonstrating its effectiveness in removing redundant heads within a layer and entire layers with similar behavior. Moreover, our method aligns with the interpretation by [Burgess et al. \(2018\)](#) suggesting that VIB encourages the acquisition of more disentangled representations.

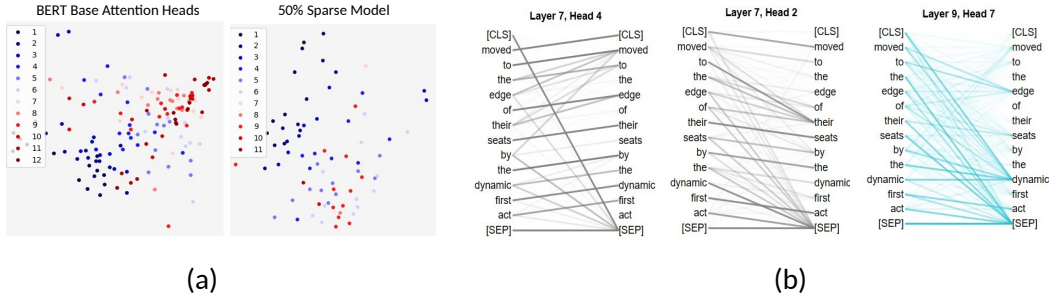


Figure 13: (a) Comparison between full BERT-base and 50% pruned model attention heads in 2-D space. Distance between points reflect average Jensen-Shannon divergences between head representations. (b) Heads in pruned model exhibit sparser, divergent behavior compared to un-pruned model. Heads retained in the 50% pruned model showing attention among input tokens from SST-2 dataset